nature climate change

LETTERS

PUBLISHED ONLINE: 30 MARCH 2015 | DOI: 10.1038/NCLIMATE2573

Equilibrium climate sensitivity in light of observations over the warming hiatus

Daniel J. A. Johansson[1]*, Brian C. O'Neill[2], Claudia Tebaldi[2] and Olle Häggström[3]

A key uncertainty in projecting future climate change is the magnitude of equilibrium climate sensitivity (ECS), that is, the eventual increase in global annual average surface temperature in response to a doubling of atmospheric CO_2 concentration. The lower bound of the likely range for ECS given in the IPCC Fifth Assessment Report (AR5; refs 1,2) was revised downwards to 1.5 °C, from 2 °C in its previous report[3], mainly as an effect of considering observations over the warming hiatus—the period of slowdown of global average temperature increase since the early 2000s. Here we analyse how estimates of ECS change as observations accumulate over time and estimate the contribution of potential causes to the hiatus. We find that including observations over the hiatus reduces the most likely value for ECS from 2.8 °C to 2.5 °C, but that the lower bound of the 90% range remains stable around 2 °C. We also find that the hiatus is primarily attributable to El Niño/Southern Oscillation-related variability and reduced solar forcing.

The hiatus has been attributed to a range of causes, including a reduction in solar forcing[4], a La Niña-like cooling of the tropical Pacific Ocean with an associated increase in Pacific Ocean heat uptake[4–7], increased ocean heat uptake in the Atlantic Ocean and Southern Ocean[8], volcanic aerosols[4,9] and anthropogenic aerosols[10]. Further, studies estimating ECS based on simple climate models and observations extending over the hiatus period have suggested an ECS at the lower end of the likely range given in IPCC AR5 (refs 1,2,11,12). However, disentangling the roles of potential causes of the hiatus from climate system properties such as the ECS is complicated by data and model limitations.

In this study we provide a new estimate of ECS, analyse the effect observations over the hiatus have had on it, and estimate the relative contribution of various factors to the temperature trend during the hiatus. Our analysis differs from previous methodologically related statistical estimates of ECS in that we distinguish observations of global mean near-land surface temperature (GMLST) from those of global mean sea surface temperature (GMSST) and use ocean heat content (OHC) observations continuous over time to a greater depth (2,000 m instead of 700 m), a potentially important addition as heat accumulation during the hiatus is thought to be particularly strong at depths below 700 m (refs 5,8,13). We also consider surface temperature variability induced by the El Niño/Southern Oscillation (ENSO; ref. 14).

By using an energy balance model and a Bayesian approach to statistics we assess how estimates of ECS change with the accumulation of historical observations, similar in some respects to studies focusing on learning about ECS over time[11,15–17]. These studies have primarily focused on the pace of learning about ECS over time in rather general terms whereas we focus on how the shape of the probability density function (PDF) of ECS changes over time as observations accumulate to analyse implications of the hiatus for estimates of ECS. This is done by progressively extending the time horizon when estimating the PDF: the model integrations all start in 1765, but end in 1986, 1991, 1996, 2001, 2006, or 2011.

The model simulations based on parameters sampled from the joint posterior PDF from the full observational history up to 2011 replicate well the observed surface temperature history, including the warming hiatus since the early 2000s (Fig. 1). The mean modelled global average surface air temperature (SAT; ref. 18) exhibits a correlation coefficient of 0.95 with observations over the period 1880–2011. As expected, the relative fit of the model to the observations improves after 1950, when observational uncertainties begin to decline significantly (see also Supplementary Figs 3 and 4).

The model generates a weak linear warming trend over the period 2002–2011 of +0.053 °C per decade (90% interval of −0.053 to 0.16 °C per decade), compared to the trend in the observations of −0.049 °C per decade (90% interval of −0.10 to 0.00 °C per decade). Both trends are substantially lower than the trend over the period 1970–2011 of about 0.16 °C per decade in both the model output and the observations. The observed temperature peak in 1998, as well as the observed temperatures in 1999 and 2000, is underestimated by the model. As a result, the modelled temperature trend over the period 1998–2011 is larger than observed (Table 1). This model behaviour has an impact on the posterior of the PDF of ECS, as we discuss further below.

A decomposition of the different key factors contributing to temperature variability indicates that the relatively flat temperature trend since 2002 is a result of an anthropogenic warming signal of about 0.19 °C per decade, an ENSO-induced cooling of about of 0.11 °C per decade and a cooling from reduced solar forcing of about 0.043 °C per decade. In addition, we find a small warming contribution from volcanic aerosols. In contrast to other studies[4], we find that the recovery from Mt Pinatubo is stronger than the cooling caused by the small volcanoes that has occurred since the early 2000s.

Differences in modelled and observed warming are expected for several reasons. Even though there is a correlation between NINO3.4 and global temperature variability (see Supplementary Section 1.8), the NINO3.4 index is not likely to capture the full global average temperature effect of ENSO. Further, other sources of internal variability are not explicitly accounted for in our analysis; they are incorporated only indirectly through the use of an autoregressive process (see Methods). Finally, the observational time series include errors and biases, including the omission of polar warming in the temperature observations[19], and models are always a simplification of the real system.

[1]Division of Physical Resource Theory, Department of Energy and Environment, Chalmers University of Technology, 412 96 Gothenburg, Sweden. [2]Climate and Global Dynamics Division, National Center for Atmospheric Research, 1850 Table Mesa Drive, 80305 Boulder, USA. [3]Department of Mathematical Sciences, Chalmers University of Technology, 412 96 Gothenburg, Sweden. *e-mail: daniel.johansson@chalmers.se

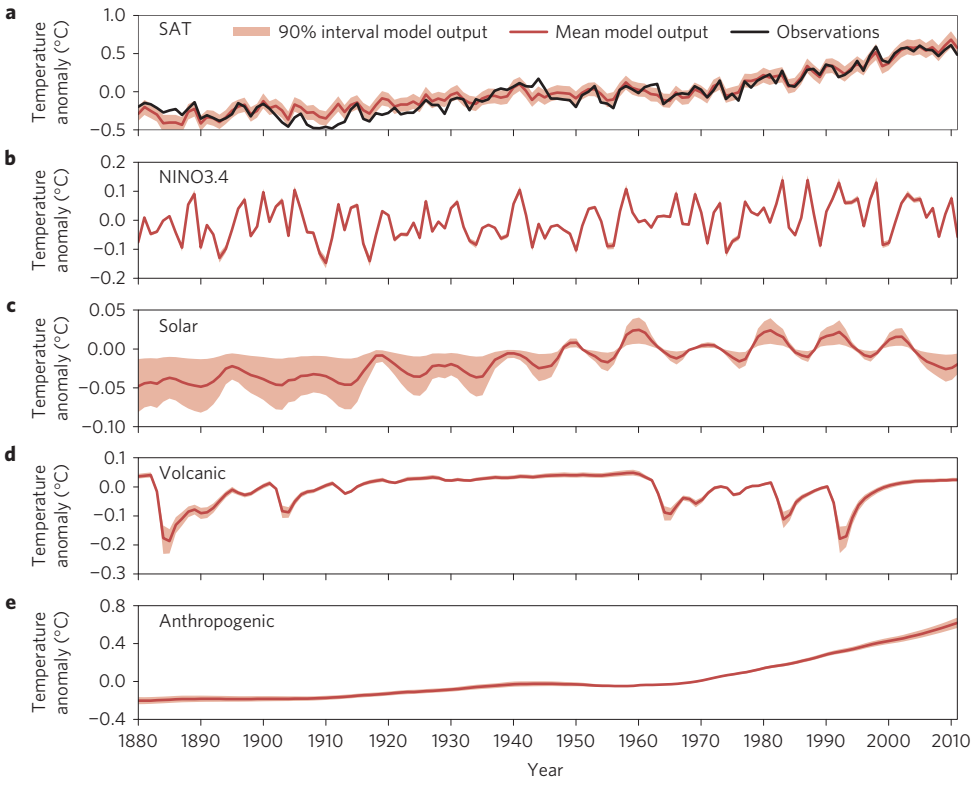

Figure 1 | Comparison between observations on SAT anomaly and corresponding model output using the posterior PDF generated by using observations up to 2011. Mean and 90% uncertainty intervals are used to characterize model output. All time series are normalized to the period 1951–1980. **a**–**d**, The SAT anomaly (**a**) is decomposed into four different contributing factors; NINO3.4 (**b**), solar irradiance (**c**), volcanic aerosols (**d**) and anthropogenic warming (**e**). The legend in **a** applies to all panels.

Table 1 | Estimates on linear temperature trend in observations and model output, including a decomposition of factors contributing to the modelled trend.

		Trend 2002–2011 (°C per decade)	Trend 1998–2011 (°C per decade)	Trend 1970–2011 (°C per decade)
NCDC SAT	Average	−0.049	0.044	0.16
	90% C.I.*	−0.10 to 0.00	0.014 to 0.073	0.155 to 0.165
Model SAT	Average	0.053	0.15	0.16
	90% C.I.	−0.053 to 0.16	0.085 to 0.22	0.14 to 0.18
Anthropogenic warming	Average	0.19	0.17	0.15
	90% C.I.	0.16 to 0.22	0.14 to 0.20	0.13 to 0.16
NINO3.4	Average	−0.11	−0.0095	0.0081
	90% C.I.	−0.12 to −0.092	−0.011 to −0.0077	0.0071 to 0.0092
Solar irradiance	Average	−0.043	−0.030	−0.0040
	90% C.I.	−0.071 to −0.012	−0.050 to −0.0084	−0.0064 to −0.0011
Volcanic aerosols	Average	0.011	0.023	0.0097
	90% C.I.	0.0064 to 0.015	0.017 to 0.031	0.0075 to 0.012
Other internal variability	Average	0.0	0.0	0.0
	90% C.I.	−0.099 to 0.099	−0.059 to 0.059	−0.011 to 0.011

*Based on the assumption that observational errors are independent and normally distributed.

Results on how the posterior estimates of the PDF of ECS change as observations accumulate show that learning about ECS is not a simple linear process (Figs 2 and 3). In general terms, the 90% uncertainty interval of the PDF narrows over time, but the path is irregular.

Using observations up to 1986 effectively eliminates the low end of the PDF of ECS. The estimated probability that ECS is below 1 °C is reduced by about an order of magnitude in comparison with the prior assumption (from 5% to about 0.5%). The probability of ECS being higher than 6 °C is also reduced substantially (from 47% to 13%), although the posterior PDF contains a long, but rather narrow, tail at the high end. This is in line with previous studies that have found that a tail for high values of ECS is difficult to reject when relatively wide (uniform) priors are used[20].

As observations accumulate, the prior assumption becomes progressively less influential on the posterior distribution. The tail at the high end of the distribution decays and eventually disappears (Figs 2 and 3). However, the learning is irregular. Adding

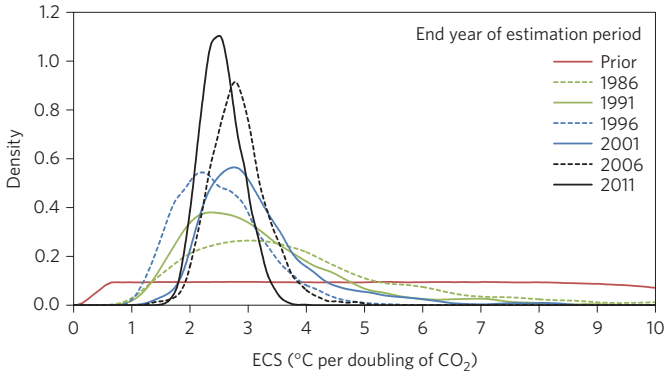

Figure 2 | The posterior marginal PDF of ECS estimated from historical observations over successively longer time periods.

observations over the period 1992–1996 causes the tail to vanish (the probability of ECS above 5 °C is less than 0.4%) and the 90% range of the PDF to drop towards lower ECS values (Fig. 3). The use of observations through 2001 causes the PDF to shift clearly to higher values and the 90% interval to widen (the probability of ECS above 5 °C increases to almost 6%).

Adding observations beyond 2001 progressively reduces the upper end of the PDF. Using observations up to 2011 effectively eliminates ECS values greater than 4 °C (with a probability of less than 0.02% of a larger ECS value; Fig. 2). The low end of the distribution is relatively more stable as observations accumulate beyond 2001, with the 5th percentile of the distribution remaining close to 2 °C (Fig. 2).

The mode of the PDF of ECS also fluctuates irregularly as observations accumulate over each five-year period (Figs 2 and 3). For example, including observations over the period 1992–1996 causes a drop in the mode, from 2.4 to 2.2 °C, whereas including observations over the period 1997–2001 causes the mode to shift up to 2.8 °C. The subsequent observations over the hiatus period cause the mode to decline to 2.5 °C by 2011.

Some explanations for these changes in the PDF of ECS are suggested by changes in the estimates for other components of the model. For example, the reduction in the ECS, particularly its high-end tail, by including data through 1996 is in part driven by the OHC observations. These observations are critical for constraining the effective vertical diffusivity (EVD), which controls ocean heat uptake in the model. EVD in turn strongly affects the estimate of ECS due to its effect on the surface energy balance[17,21] (see also Supplementary Section 3). As the OHC observations are available only since 1957, additional observations have an important role in constraining the EVD. The additional ten years of observations from 1987 to 1996 are especially important because the measurement uncertainty declines over this period of time and the observations are less variable after the mid-1980s (see Supplementary Figs 5 and 9). As a consequence the PDF of EVD shrinks as observations accumulate beyond 1986 (Fig. 3), which also leads to a smaller spread in the PDF of ECS.

The explanation behind the shift in the PDF of ECS towards higher values and the widening of the 90% interval that occurs when adding observation over the period 1997–2001 relates to the strong El Niño in 1997/1998. The model underestimates the SAT during this period of time (Fig. 1) for at least three possible reasons. First, there are uncertainties in the relationship between NINO3.4 and SAT fluctuations (see Methods and Supplementary Section 1.8 for more information about assumptions). Second, the NINO3.4 index may underestimate the strength of this El Niño event relative to other events. The peak in the NINO3.4 index in 1997/1998 is relatively weak; another ENSO index (NINO12) shows a much stronger peak (see Supplementary Fig. 2). Third, other modes of

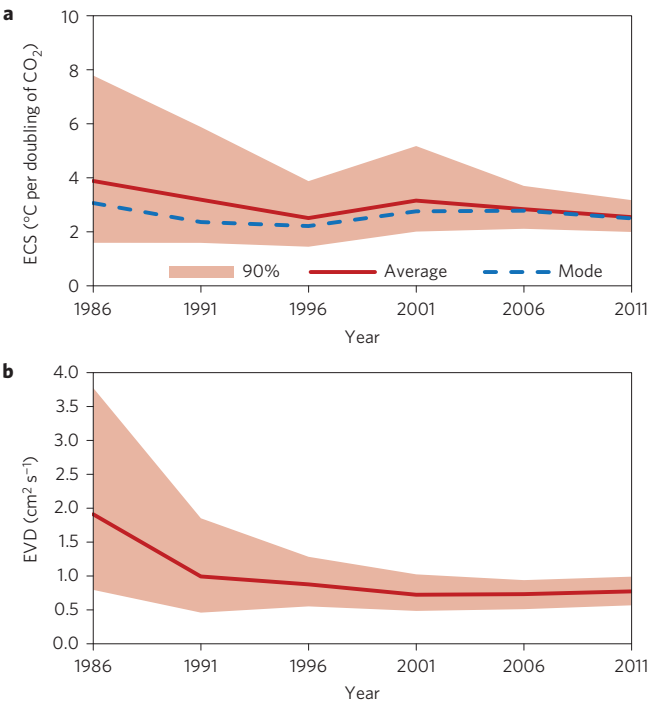

Figure 3 | Characteristics of PDFs of ECS and EVD as observations accumulates. a,**b**, Time profile for the mean, mode (for ECS only) and 90% credible interval of the marginal PDF of ECS (**a**) and EVD (**b**).

internal variability, including variability with longer periodicity than ENSO, may have contributed to the observed temperature peak during this period of time. Hence, the NINO3.4 index is probably not picking up all the El Niño effects and misses other sources of natural variability that may have played a role; instead, some portion of those effects show up as an increase in the ECS estimate.

The 90% interval of the posterior PDF of ECS obtained when using observations up to 2011 is 2.0 to 3.2 °C. This estimated width of the PDF of ECS may be on the low side. We do not explicitly address potentially important issues such as multi-decadal timescale internal variability, uncertainty in the shape of the forcing time series and the autocorrelation of the observational errors. Inclusion of these features in the analysis could have increased the width of the PDF.

Some of the key assumptions in our model are addressed in a sensitivity analysis. We find that our estimate of the PDF of ECS is dependent on the inclusion of NINO3.4 as an independent regression covariate, a key difference in our analysis compared to several other related studies[1,2,12,15,16]. The 90% credible interval grows and becomes 2.1 °C to 3.8 °C if NINO3.4 is not included in the analysis. Further, some studies[16] do no not use exogenous estimates on observational errors when estimating PDFs of ECS. If we also neglect such estimates the posterior PDF of ECS shifts to higher values and becomes even wider (90% interval being 2.3 °C to 4.3 °C). Our estimated PDF of ECS is, as discussed above, also affected by the use of OHC observations. If these are neglected the 90% interval for the PDF of ECS is 2.8 °C to 9.0 °C. We also find that the posterior PDF of ECS shifts towards lower values, whereas the width remains about the same, if OHC observations down to 700 m are used instead of observations down to 2,000 m. The PDF of ECS is relatively insensitive if we use global aggregated surface temperature observations instead of separated land and sea surface temperature observations.

Finally, although we find that the inclusion of observations over the hiatus period contributes to a more constrained estimate of ECS, the degree to which this was due to the hiatus per se, as opposed to

the accumulation of more data in general, is unclear. In addition, we also find that the PDF of ECS shifts back and forth as observations accumulate. This indicates that unforced natural variability plays a key role for the estimate of the PDF of ECS (ref. 15). Such shifts in the PDFs can sometimes move in directions which retrospectively turn out to be incorrect—that is, we have negative learning[22,23]. Further, limitations and uncertainties in the structural relationships in geophysical models as well in statistical models hamper any observationally based estimate of ECS, implying that all empirical estimates of ECS should be interpreted with some care. For these reasons we suggest that it is too early to conclude that the hiatus has had any particular impact on estimates of ECS.

Methods

To model forced temperature response we use a land–ocean resolved upwelling diffusion energy balance model (UDEBM). The model, and the use of such models in statistical modelling, is described at greater length in Supplementary Section 1. The UDEBM is forced by estimates of effective radiative forcing (RF) over the period 1765–2011, based on ref. 24 for anthropogenic sources (http://www.pik-potsdam.de/~mmalte/rcps/), ref. 25 for Solar RF, and refs 26,27 for volcanic aerosol RF (http://hurricane.ncdc.noaa.gov/pls/paleox/f?p=519:1:0::::P1_STUDY_ID:14168 and http://data.giss.nasa.gov/modelforce/strataer, respectively).

Posterior PDFs are calculated based on Bayes theorem

$$p(\theta|y) \propto L(y|\theta) \cdot p(\theta)$$

where $p(\theta)$ is the prior probability density for parameters θ, $L(y|\theta)$ is the likelihood function, and $p(\theta|y)$ is the posterior probability density for the parameters θ conditional on observations y. The likelihood function is the probability density of the observations y conditional on the parameters θ; for our application, it is a measure of how well the model with specific parameter combinations replicates the observations, accounting for internal variability and observational error. The statistical methodology is explained in more detail in Supplementary Section 1.

The model is constrained by observations on GMSST and GMLST (ref. 18) (ftp://ftp.ncdc.noaa.gov/pub/data/mlost/operational/products) and OHC above 2,000 m (ref. 28) (http://www.nodc.noaa.gov/OC5/3M_HEAT_CONTENT).

The UDEBM does not generate internal variability. To compensate for this the variability induced by ENSO is captured by making the modelled GMSST and GMLST dependent on the NINO3.4 index lagged by two months and six months, respectively. The lag is estimated by maximizing the correlation between the residual of temperature observations minus the modelled temperature output (calculated without considering the global temperature impact of ENSO) and the lagged NINO3.4 index (Supplementary Section 1.8). The NINO3.4 index is based on the NOAA Extended Reconstructed Sea Surface Temperature (SST) V3b (http://climexp.knmi.nl/selectindex.cgi). Remaining natural variability in GMLST, GMSST and OHC is assumed to follow a first-order autoregressive (AR1) process, with the autocorrelation and variance estimated from the residuals between the modelled and observed variables (Supplementary Section 2.1–2.3).

The prior probability density distributions are either uniform, normal, truncated normal or lognormal. We consider the following EBM parameters to be probabilistic: climate sensitivity parameter, effective mixed layer depth, effective vertical diffusivity, upwelling rate, relative warming of sinking polar water to global mean sea surface warming and equilibrium land–sea surface warming ratio. The priors for all of these parameters are assumed to be uniformly distributed, with the exception of the equilibrium land–sea surface warming ratio, for which we assume a normal distribution based on output from climate system models[2]. The prior scaling factors for relating the NINO3.4 index to GMSST and GMLST variability and the parameters of the AR(1) processes are uniform and set wide enough to not constrain the posterior estimate. The paths of the different effective radiative forcing contributions (for CO_2, CH_4, N_2O, tropospheric O_3, anthropogenic aerosols, solar, and volcanic aerosols) are fixed, but the magnitudes are scaled with probabilistically treated scaling factors. The prior distributions for scaling parameters for historical effective radiative forcing time series are assumed to be normal, truncated normal or lognormal, with standard deviations that approximately correspond to the effective radiative forcing uncertainty reported in IPCC AR5 (ref. 25). However, the prior scaling factor for volcanic aerosol forcing is based on ref. 29. The forcing estimates and their prior uncertainties are estimated from climate system models, these are primarily not constrained by observations on the global energy balance; hence there should be no major problems of circular reasoning. See Supplementary Section 1.7 for further information about priors.

The posterior PDF is estimated through the use of a Markov Chain Monte Carlo (MCMC) approach using the Metropolis algorithm[30]. We take 500,000 samples when estimating the posterior PDF for each model set-up, with set-ups differing with regard to the end-year of the observational record used. The proposal distribution for the Metropolis algorithm is a random walk. A new sample for all the uncertain model parameters is taken simultaneously in each proposal. The first 20,000 samples of the posterior distribution are used as 'burn-in'; that is, they are discarded, and only the subsequent MCMC samples are used to estimate the posterior distribution. Every twentieth sample of the chain is retained, and the PDFs presented in Fig. 2 are estimated from the samples by using a normally distributed kernel function.

The decomposition presented in Fig. 1, and the subsequent estimation of the linear temperature trend due to the different factors presented in Table 1, are constructed by running the UDEBM with only one specific forcer/mechanism at a time. The estimated temperature contribution for each forcer/mechanism is based on 1,000 samples of the posterior PDF estimated when using observations up to 2011. Running the model with only one specific forcer/mechanism at a time is valid because the forcing response in the UDEBM is linear. Hence, the sum of the temperature contributions of each forcer/mechanism is equal to the temperature response of the sum of the forcers/mechanisms.

Received 9 September 2014; accepted 3 February 2015; published online 30 March 2015; corrected online 14 April 2015; corrected after print 10 June 2015

References

1. Bindoff, N. L. *et al.* in *Climate Change 2013: The Physical Science Basis* (eds Stocker, T. F. *et al.*) 867–952 (IPCC, Cambridge Univ. Press, 2013).
2. Collins, M. *et al.* in *Climate Change 2013: The Physical Science Basis* (eds Stocker, T. F. *et al.*) 1029–1136 (IPCC, Cambridge Univ. Press, 2013).
3. Meehl, G. A. *et al.* in *Climate Change 2007: The Physical Science Basis* (eds Solomon, S. *et al.*) 747–845 (IPCC, Cambridge Univ. Press, 2013).
4. Huber, M. & Knutti, R. Natural variability, radiative forcing and climate response in the recent hiatus reconciled. *Nature Geosci.* **7,** 651–656 (2014).
5. Meehl, G. A., Arblaster, J. M., Fasullo, J. T., Hu, A. & Trenberth, K. E. Model-based evidence of deep-ocean heat uptake during surface-temperature hiatus periods. *Nature Clim. Change* **1,** 360–364 (2011).
6. Kosaka, Y. & Xie, S-P. Recent global-warming hiatus tied to equatorial Pacific surface cooling. *Nature* **501,** 403–407 (2013).
7. Trenberth, K. E. & Fasullo, J. T. An apparent hiatus in global warming? *Earth's Future* **1,** 19–32 (2013).
8. Chen, X. & Tung, K-K. Varying planetary heat sink led to global-warming slowdown and acceleration. *Science* **345,** 897–903 (2014).
9. Santer, B. D. *et al.* Volcanic contribution to decadal changes on tropospheric temperature. *Nature Geosci.* **7,** 185–189 (2014).
10. Kaufmann, R. K., Kauppi, H., Mann, M. L. & Stock, J. H. Reconciling anthropogenic climate change with observed temperature 1998–2008. *Proc. Natl Acad. Sci. USA* **108,** 11790–11793 (2011).
11. Aldrin, M. *et al.* Bayesian estimation of climate sensitivity based on a simple climate model fitted to observations of hemispheric temperatures and global ocean heat content. *Environmetrics* **23,** 253–271 (2012).
12. Otto, A. *et al.* Energy budget constraints on climate response. *Nature Geosci.* **6,** 415–416 (2013).
13. Balmaseda, M. A., Trenberth, K. E. & Källén, E. Distinctive climate signals in reanalysis of global ocean heat content. *Geophys. Res. Lett.* **40,** 1754–1759 (2013).
14. Trenberth, K. E., Caron, J. M., Stepaniak, D. P. & Worley, S. The evolution of ENSO and global atmospheric surface temperatures. *J. Geophys. Res.* **107,** http://dx.doi.org/10.1029/2000JD000298 (2002).
15. Huber, M., Beyerle, U. & Knutti, R. Estimating climate sensitivity and future temperature in the presence of natural climate variability. *Geophys. Res. Lett.* **41,** 2086–2092 (2014).
16. Urban, N. M., Holden, P. B., Edwards, N. R., Sriver, R. L. & Keller, K. Historical and future learning about climate sensitivity. *Geophys. Res. Lett.* **41,** 2543–2552 (2014).
17. Skeie, R. B., Berntsen, T., Aldrin, M., Holden, M. & Myhre, G. A lower and more constrained estimate of climate sensitivity using updated observations and detailed radiative forcing time series. *Earth Syst. Dynam.* **5,** 139–175 (2014).
18. Smith, T. M., Reynolds, R. W., Peterson, T. C. & Lawrimore, J. Improvements to NOAA's historical merged land–ocean surface temperature analysis (1880–2006). *J. Clim.* **21,** 2283–2296 (2008).
19. Cowtan, K. & Way, R. G. Coverage bias in the HadCRUT4 temperature series and its impact on recent temperature trends. *Q. J. R. Meteorol. Soc.* **140,** 1935–1944 (2014).
20. Annan, J. D. & Hargreaves, J. C. On the generation and interpretation of probabilistic estimates of climate sensitivity. *Climatic Change* **104,** 423–436 (2011).
21. Forest, C. E., Stone, P. H., Sokolov, A. P., Allen, M. R. & Webster, M. D. Quantifying uncertainties in climate system properties with the use of recent climate observations. *Science* **295,** 113–117 (2002).

22. Oppenheimer, M., O'Neill, B. C. & Webster, M. Negative learning. *Climatic Change* **89,** 155–172 (2008).
23. Hannart, A., Ghil, M., Dufresne, J-L. & Naveau, P. Disconcerting learning on climate sensitivity and the uncertain future of uncertainty. *Climatic Change* **119,** 585–601 (2013).
24. Meinshausen, M. *et al.* The RCP greenhouse gas concentrations and their extension from 1765 to 2300. *Climatic Change* **109,** 213–241 (2011).
25. Myhre, G. *et al.* in *Climate Change 2013: The Physical Science Basis* (eds Stocker, T. F. *et al.*) 659–740 (IPCC, Cambridge Univ. Press, 2013).
26. Crowley, T. J. & Unterman, M. B. Technical details concerning development of a 1200-yr proxy index for global volcanism. *Earth Syst. Sci. Data* **5,** 187–197 (2013).
27. Sato, M., Hansen, J. E., McCormick, M. P. & Pollack, J. B. Stratospheric aerosol optical depth, 1850–1990. *J. Geophys. Res.* **98,** 22987–22994 (1993).
28. Levitus, S. *et al.* World ocean heat content and thermosteric sea level change (0–2000 m) 1955–2010. *Geophys. Res. Lett.* **39,** L10603 (2012).
29. Tomassini, L., Reichert, P., Knutti, R., Stocker, T. F. & Borsuk, M. E. Robust Bayesian uncertainty analysis of climate system properties using Markov chain Monte Carlo methods. *J. Clim.* **20,** 1239–1254 (2007).
30. Gelman, A. *et al. Bayesian Data Analysis* (Chapman & Hall/CRC, 2004).

Acknowledgements

D.J.A.J. wants to thank the Swedish Energy Agency and Carl Bennet AB for financial support. C.T. was supported by the Regional and Global Climate Modeling Program (RGCM) of the US Department of Energy's Office of Science (BER), Cooperative Agreement DE-FC02-97ER62402. O.H. was supported by the Knut and Alice Wallenberg Foundation and the Swedish Research Council. C. Azar is acknowledged for useful comments.

Author contributions

D.J.A.J. designed and performed the research with input from the other authors. All authors contributed to writing the paper.

Additional information

Supplementary information is available in the online version of the paper. Reprints and permissions information is available online at www.nature.com/reprints. Correspondence and requests for materials should be addressed to D.J.A.J.

Competing financial interests

The authors declare no competing financial interests.

CORRIGENDUM

Equilibrium climate sensitivity in light of observations over the warming hiatus

Daniel J. A. Johansson, Brian C. O'Neill, Claudia Tebaldi and Olle Häggström

Nature Climate Change http://dx.doi.org/10.1038/nclimate2573 (2015); published online 30 March 2015; corrected online 14 April 2015

In the version of this Letter originally published, in the third paragraph, the section of text including 'Our analysis differs... at depths below 700m (refs 5,8,13).' was unclear and should have been:

'Our analysis differs from previous methodologically related statistical estimates of ECS in that we distinguish observations of global mean near-land surface temperature (GMLST) from those of global mean sea surface temperature (GMSST) and use ocean heat content (OHC) observations continuous over time to a greater depth (2,000m instead of 700 m), a potentially important addition as heat accumulation during the hiatus is thought to be particularly strong at depths below 700m (refs 5,8,13).'

Further, in the Methods section, radiative forcing should have been described as effective radiative forcing. These errors have been corrected in all versions of the Letter.

CORRIGENDUM

Equilibrium climate sensitivity in light of observations over the warming hiatus

Daniel J. A. Johansson, Brian C. O'Neill, Claudia Tebaldi and Olle Häggström

Nature Clim. Change **5,** 449–453 (2015); published online 30 March 2015; corrected after print 10 June 2015

In the version of this Letter originally published, ref. 9 was incorrectly cited twice; the sentence including the second occurrence should have read: "In contrast to other studies[4], we find that the recovery from Mt Pinatubo is stronger than the cooling caused by the small volcanoes that has occurred since the early 2000s." This error has been corrected in the online versions of the Letter.